2021 43rd Annual International Conference of the
IEEE Engineering in Medicine & Biology Society (EMBC)
Oct 31 - Nov 4, 2021. Virtual Conference

Magnetic Resonance Imaging compatible Elastic Loading Mechanism (MELM): A minimal footprint device for MR imaging under load

Jaap Boon [1], Telly Ploem [1], Cole S. Simpson [2], Ingo Hermann [1,3], Mehmet Akçakaya [4], Edwin H. Oei [5], Amir A. Zadpoor [6], Nazli Tümer [6], Tom M. Piscaer [7], Joao Tourais [1] and Sebastian Weingärtner [1]

***Abstract*— Quantitative Magnetic Resonance Imaging (MRI) can enable early diagnosis of knee cartilage damage if imaging is performed during the application of load. Mechanical loading via ropes, pulleys and suspended weights can be obstructive and require adaptations to the patient table. In this paper, a new lightweight MRI-compatible elastic loading mechanism is introduced. The new device showed sufficient linearity ($|\alpha/\beta| = 0.42 \pm 0.25$), reproducibility (CoV = $5 \pm 2\%$), and stability (CoV = $0.5 \pm 0.1\%$). In vivo and ex vivo scans confirmed the ability of the device to exert sufficient force to study the knee cartilage under loading conditions, inducing up to a 29% decrease in T_2^* of the central medial cartilage. With this device mechanical loading can become more accessible for researchers and clinicians, thus facilitating the translational use of MRI biomarkers for the detection of cartilage deterioration.**

I. INTRODUCTION

In the United States, knee osteoarthritis (OA) is the most prevalent joint disorder and affects up to 13% of people aged 60 and older [1]. Due to the aging population and persisting obesity epidemic, the number of people affected with OA is steadily increasing [1]. Cartilage deterioration is a hallmark of OA and early detection is key to allow for intervention before irreversible damage occurs [2].

Quantitative Magnetic Resonance Imaging (qMRI) may enable early diagnosis of knee cartilage alteration when imaging is performed during the application of load to the joint. Several studies have reported an abnormal response in MRI-related tissue relaxation times when load is applied to the diseased knee [3][4][5][6][7][8]. However, these measurements are currently only feasible with complex MRI compatible loading devices and, thus, are limited to the research setting. Most previous studies have used combinations of ropes and pulleys that were able to apply load with suspended weights [3][4][5][6][7][8]. While those settings showed reproducible loading in the relevant range, modifications of the MRI setup and fixture to the patient tables are required [9]. The setups are also obtrusive and reduce space within the confined MRI bore. As the lack of space is one of the most frequently named factors for patient discomfort in an MRI, this reduces the clinical translatability of these approaches [10].

In this work, we sought to develop a new loading mechanism that is minimally obtrusive in the MRI setting and allows for portability and compatibility with conventional clinical setups. The mechanical properties of the device are studied in benchtop experiments, and the feasibility is evaluated with quantitative MRI in an ex vivo porcine knee joint and in a healthy subject, in vivo.

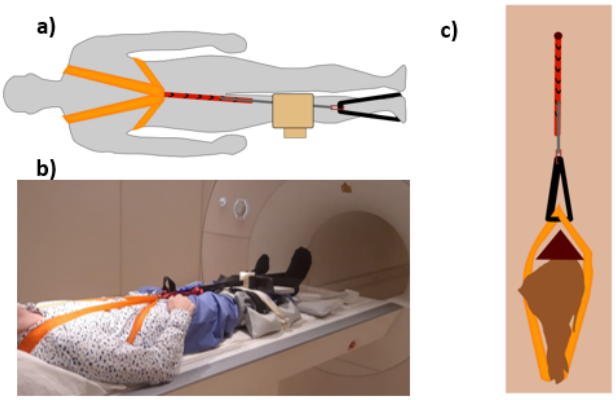

Fig. 1: a) Schematic illustration of the MELM. Loading force is applied via the extension of a rubber band. This is anchored against the subject's upper body using a harness. An adjustable strap is integrated to adjust for subject height, and a daisy chain is used to extend the rubber band with identical increments. b) The MELM worn by a human subject in the MRI. c) Schematic top view of the extended setup, animal MELM, used to apply load to a porcine joint.

II. METHODS

A. MRI compatible Elastic Loading Mechanism (MELM)

The MELM is a wearable device that connects the upper body to a force applying rubber band wrapped around the foot of the subject, as illustrated in Fig. 1a. The load is applied on the sole of the foot, using the extension of a band made of natural rubber (latex). The tension is anchored at the shoulders of the subject, using a heavy-lifting harness to achieve symmetric load distribution across both shoulders. Belts connect the upper and lower body parts to allow for

*This work was not supported by any organization
*This study was approved by the Human Research Ethics Committee of the TU Delft

[1]Department of Imaging Physics, Delft University of Technology, Delft, The Netherlands https://www.mars-lab.eu/
[2]Department of Mechanical Engineering, Stanford University, Stanford, CA, USA
[3]Computer Assisted Clinical Medicine lab, Medical Faculty Mannheim, Heidelberg University, Mannheim, Germany
[4]Department of Electrical and Computer Engineering, and Center for Magnetic Resonance Research, University of Minnesota, Minneapolis, MN, United States
[5]Department of Radiology & Nuclear Medicine, Erasmus University Medical Center, Rotterdam, The Netherlands
[6]Department of Biomechanical Engineering, Delft University of Technology, Delft, The Netherlands
[7]Department of Orthopaedic Surgery, Erasmus University Medical Center, Rotterdam, The Netherlands

adjustable and reproducible loading. These belts include: (1) an adjustable strap that compensates for differences in the subject height and (2) a daisy chain used to extend the rubber band by identical increments for all subjects. The adjustable strap is attached to different loops of the daisy chain using a custom printed polylactic acid hook. A 48 cm long rubber band with a cross-sectional area of 6×0.4 cm^2 is used. When folded around the foot, both sides measure 23 cm when no force is applied. The daisy chain allows for 14 discrete length settings for the elastic band with a 7 cm increment size.

The setup was also adapted to facilitate ex vivo animal experiments. The daisy chain of the MELM was mounted to a pole on a wooden support plank. An object holder was placed at a distance from the pole. Different mounts can be attached to the object holder to allow for fixture of the ex vivo specimen. The harness is wrapped around the specimen and attached to the rubber band. Straps connect the rubber band to the daisy chain. A schematic depiction of the extended setup is shown in Fig. 1c.

A bill of materials, design files for the 3D printed components and instructional videos for assembly can be found at `https://gitlab.tudelft.nl/mars-lab/melm`.

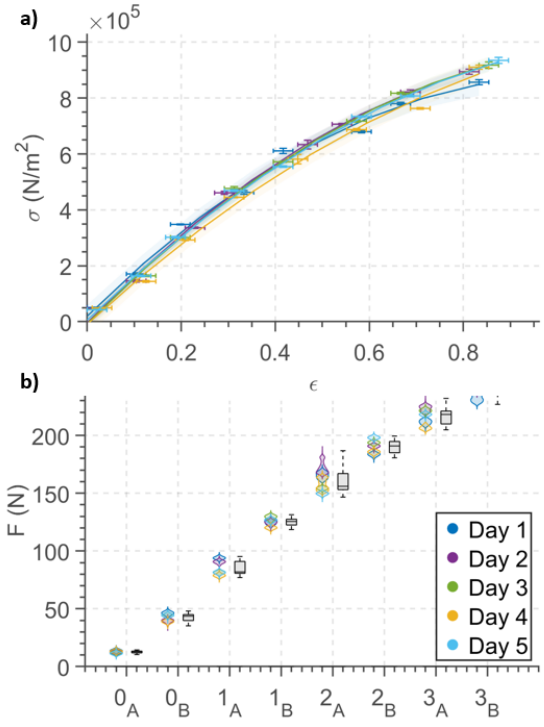

Fig. 2: Properties of the banchtop experiment, measured on 5 consecutive days. a) The relationship between stress σ [N/m^2] and strain ϵ [-]. b) Each measurement day shows a violin plot of the measured force F (N) for 2x4 increments. One half of the increments (labeled with subscript A) was initialised at 13±1 N and and the other half (labeled with subscript B) was initialised at 43±3 N. Next to the violin plots are boxplots that show the minimum, interquartile range, mean and maximum for all measurement days.

B. Material Evaluation

The MELM was evaluated in bench-top experiments for its ability to reproducibly exert force. Forces were measured in two sets of four increments, each. The first set was initialized at 13 ± 1 N in the first loop and the second one at 42 ± 3 N. Experiments were repeated on five consecutive days for 10 minutes. The rubber material was characterized by its stress-strain relation, where stress σ was derived from the force measurement F and the cross-sectional area A, as $\sigma = F/A$. To study the linearity of the stress strain curves, second-order polynomials ($\alpha\epsilon^2 + \beta\epsilon + \gamma$) were fitted to the measurement data. $|\alpha/\beta|$ was used as a linearity measure. Statistical significance was evaluated using t-statistics, p values less than 0.05 were considered significant.

Thin flexible force sensors (FlexiForce A201 45kg, Tekscan, Boston, MA, USA) were used to measure forces within the setup for validation outside the MRI. Force measurements are reported as mean and standard deviation across measurement days, and reported as $\mu \pm SD$. Reproducibility is evaluated by the coefficient of variation (CoV) of the load at the 8 different increments across different days.

C. Ex vivo study

Ex vivo imaging was performed on a 3T scanner (Ingenia, Philips, Amsterdam, The Netherlands). The porcine knee joint originated from a female animal, 5-6 months old, with an approximate weight of 80kg. Quantification of the ex vivo cartilage was performed using a multi-parametric echo-planar imaging based magnetic resonance fingerprinting technique (MRF-EPI [11][12]) with the following imaging parameters: 0.8×0.8 mm^2 in-plane resolution, 32 slices, 2 mm slice thickness, 2 mm slice gap, TE 17-77.5 ms, FA: 34-86°, 3.5 minutes scan-time. Four regions of interest (ROIs) were manually defined: the central medial femoral cartilage (CMF), the central lateral femoral cartilage (CLF), the central medial tibial cartilage (CMT), and the central lateral tibial cartilage (CLT). ROIs were drawn across two consecutive slices and T_2^* values are reported as the mean and standard deviation across these slices. Imaging was performed before loading, and 4 times for each applied load, with 3.6±0.1 min in between each image.

D. In vivo study

Reproducibility and stability of the in vivo forces were studied in one healthy subject (male, 23 years) outside the MRI suite. Forces were measured on three separate days for four different extensions, initialized at 25±4 N. Reproducibility was evaluated as CoV across the measurements. To measure the stability of the setup, forces were measured at the highest load (third increment) on five separate days. Stability was evaluated as the cross-time CoV throughout one experiment, averaged across all measurement days.

In vivo imaging was performed in a second center at 3T (Magnetom Prisma, Siemens Healthineers, Erlangen Germany). One healthy male human volunteer was enrolled in this study (29 years, 61 kg, BMI 19.7). Imaging was performed using the same MRF-EPI sequence with the

following parameters: 0.8×0.8 mm^2 in-plane resolution, 31 axial slices, 2 mm slice gap, TE 19-79.5 ms, FA: 34-86 deg, 2.5 minutes scan-time. Images were obtained axially and reformatted to sagittal views for evaluation. Two ROIs were manually defined: the central medial cartilage (CM) and the central lateral cartilage (CL). For three consecutive slices the T_2^* values are obtained within both ROIs. In vivo imaging was performed before loading, and 4-6 times for each applied load. An average of 2.5± 0.1 min passed between each image.

III. RESULTS

A. Material evaluation

Fig. 2a depicts the stress and strain relationship of the rubber band. Polynomial fitting revealed a linear stress-strain regime for small strain. Stress and strain strongly correlated, with high statistical significance ($R^2 = 0.9836$, $p = 10^{-30}$). The fit parameters across the five days were $\alpha = (-7.0 \pm 3.9) \cdot 10^5$ Nm^{-2}, $\beta = (16.5 \pm 3.4) \cdot 10^5$ Nm^{-2} and $\gamma = (0.0 \pm 0.5) \cdot 10^5$ Nm^{-2}. Polynomial fitting revealed a significant (p=0.0028), but small non linear contribution ($|\alpha/\beta| = 0.42 \pm 0.25$). Fig. 2b shows forces F for 2x4 increments over five days for the bench-top experiments. The setup achieved a day-to-day reproducibility with a CoV of $5 \pm 2\%$. For the animal MELM, the applied forces were: no load, 85±1 N, 159±3 N and 215±2 N, with an average load increment of 71 N.

B. Ex vivo study

Fig. 3 shows example T_2^* maps acquired in the pig knee before and after loading, along with the lateral ROIs. Spatially localized T_2^* decreases are apparent, particularly in the lateral femoral region. Quantitative T_2^* before loading

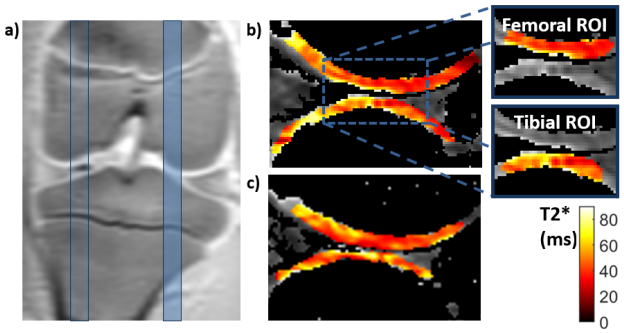

Fig. 3: a) Coronal cross-section of the structural image of the porcine knee. The two blue rectangles indicate the approximate slice positions used for data analysis of the medial and lateral cartilage. The lateral slices are highlighted. b) Quantitative T_2^* map of the fully segmented lateral cartilage under no load. The color overlay in the inset illustrates the femoral and tibial ROI positions. c) Quantitative T_2^* map of the fully segmented lateral cartilage under 159±3 N of load.

inside the MT, MF, LT, and LF ROIs were 24.4 ± 5.9 ms, 29.3±11.5 ms, 44.4±8.6 ms and 44.3±15.0 ms respectively. The relative change of the pig cartilage T_2^* between no load and loading conditions is reported in Table I. A consistent decrease of T_2^* is observed for all ROIs.

C. In vivo study

Fig. 4a shows measured force using 4 increments in the in vivo setup: no load, 76±6 N, 139±7 N and 199±8 N. Low temporal variability of the load over time was observed, resulting in a CoV of $0.5 \pm 0.1\%$ (Fig. 4b). Fig. 5 shows an

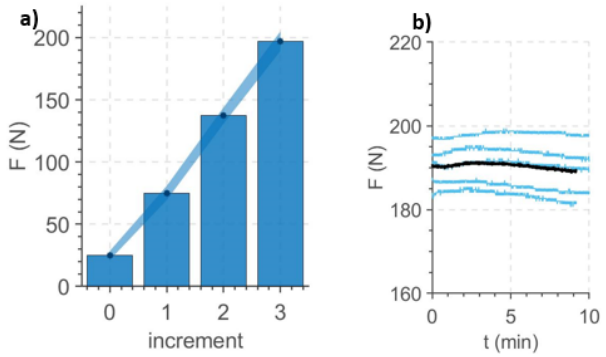

Fig. 4: a) Applied force for the in vivo setup at different increments of the daisy chain. b) Force as a function of time t (min) while the highest load (third increment) is applied. The black line indicated the mean across days.

exemplary T_2^* map acquired in the healthy volunteer when no loading was applied, along with the manually drawn medial ROI. Both the tibial and femoral cartilage were incorporated into each ROI, because of the limited spatial resolution. T_2^* before loading for the medial ROI and the lateral ROI was 25.3 ± 9 ms and 22.8 ± 13.4 ms, respectively. The relative change of cartilage T_2^* for all ROIs and loading conditions is reported in Table I. A consistent decrease in T_2^* was observed at increased loading. Furthermore, at constant load, progressively decreasing T_2^* times were measured (Fig. 6).

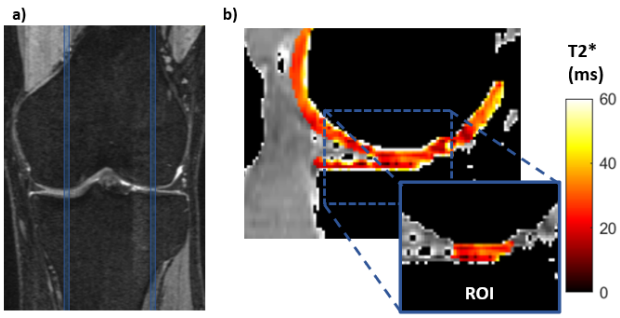

Fig. 5: a) Coronal cross-section of the structural image of the knee of the human subject. The two blue rectangles indicate the approximate slice positions used for data analysis of the medial and lateral cartilage. Each rectangle comprises three slices with 2 mm spacing. b) Quantitative T_2^* maps of the fully segmented medial cartilage under no load. The colorful overlay in the inset illustrates the exact ROI position.

IV. DISCUSSION

In this study, a new MRI-compatible elastic loading mechanism (MELM) was introduced and tested. The proposed device enabled imaging of the knee cartilage under loading conditions with minimal footprint in the MRI scanner. The device is highly portable and requires no fixtures to the MRI

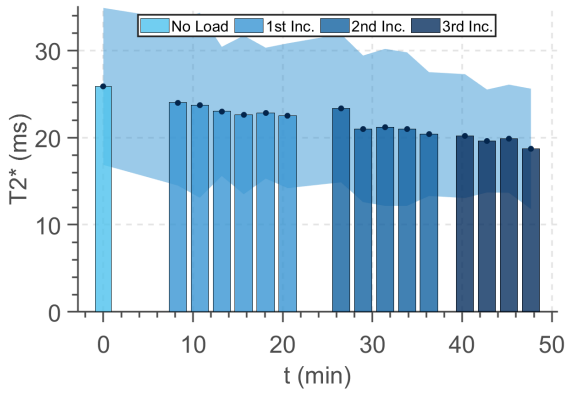

Fig. 6: Cartilage T_2^* (ms) as a function of time t (min) inside the medial ROI in vivo. The first bar corresponds to no loading. After about 8 minutes, a series of six images were acquired at 76±6 N load. Next, five images were acquired at 139±7 N, followed by four images at 199±8 N load.

TABLE I: T_2^* values and their relative change for three different loads.

ROI	Porcine T_2^* (ms)			
CMF	29.3 ± 11.5	29.3 ± 9.8	25.7 ± 9.0	22.3 ± 6.8
Δ		(-0%)	(-13%)	(-24%)
CMT	24.4 ± 5.9	25.4 ± 7.1	23.8 ± 6.2	19.7 ± 3.9
Δ		$(+4\%)$	(-3%)	(-19%)
CLF	44.3 ± 15.0	42.7 ± 10.2	39.1 ± 9.2	35.3 ± 8.7
Δ		(-4%)	(-10%)	(-19%)
CLT	44.4 ± 8.6	40.9 ± 7.1	36.6 ± 5.7	35.4 ± 8.4
Δ		(-8%)	(-18%)	(-20%)
Load [N]	0	85 ± 1	159 ± 3	215 ± 2
ROI	In Vivo T_2^* (ms)			
CM	25.3 ± 9.0	22.8 ± 8.4	20.4 ± 6.7	17.8 ± 7.7
Δ		(-10%)	(-19%)	(-29%)
CL	22.8 ± 13.4	20.7 ± 9.5	19.6 ± 12.1	17.5 ± 7.7
Δ		(-9%)	(-14%)	(-23%)
Load [N]	0	76 ± 6	139 ± 7	199 ± 8

setup. In vivo and ex vivo scans confirmed the ability of the device to exert sufficient force to study the knee under relevant loading conditions.

Rubber was selected as a material to apply load at the sole of the foot of a subject, due to its low elastic modulus and high maximal strain. The setup can be adapted to apply larger loads by using thicker or shorter rubber bands. As the rubber band is anchored against the upper body, the resulting load may be subject to slight variations during breathing. Abdominal breathing is advised for better stability.

The stress-strain analysis demonstrated operation in a largely linear regime. The sub-linear saturation at high strains up to 100% is expected for rubber [16].

The observed decrease in T_2^* is well in line with multiple studies reporting a drop in T_2 and T_{1rho} under loading[9][13][14][15]. Furthermore, the trend of further decreasing relaxation times while the loading is maintained, is in good agreement with previously reported temporal trends [15].

Unlike previous loading devices, the MELM is highly portable and can therefore be used across multiple MRI systems. Furthermore, the subject can be prepared outside the scanner room, shortening the scan preparation time and maximizing the scan time efficiency. Finally, the MELM is affordable and easy to build, with detailed instructions online to provide high reproduciblity in the final device.

V. CONCLUSION

An MRI-compatible elastic loading mechanism (MELM) to stably and reproducibly apply several increments of load inside an MRI was introduced. The MELM can be applied in vivo and on ex vivo animal specimens, and provides a portable, minimally obtrusive set-up that may improve the translation of knee MRI during loading in research and clinical settings.

REFERENCES

[1] Y. Zhang and J.M. Jordan. “Epidemiology of osteoarthritis.” Clinics in geriatric medicine vol. 26, 2010.

[2] T.J Mosher and B.J. Dardzinski. “Cartilage MRI T2 relaxation time mapping: overview and applications . ” Semin Musculoskelet Radiology, 2004.

[3] R. Patel et al. “Loaded versus unloaded magnetic resonance imaging (MRI) of the knee: Effect on meniscus extrusion in healthy volunteers and patients with osteoarthritis.” Elsevier, 2016.

[4] R.B. Souza et al. “Response of knee cartilage T1rho and T2 relaxation times to in vivo mechanical loading in individuals with and without knee osteoarthritis.” Osteoarthritis Research Society International, 2014.

[5] K. Subburaj, R.B. Souza, C. Stehling et al. “Association of MR relaxation and cartilage deformation in knee osteoarthritis.” Journal of Orthopaedic Research, 2012.

[6] K. Subburaj, R.B. Souza et al. “Changes in MR relaxation times of the meniscus with acute loading: An in vivo pilot study in knee osteoarthritis.” Journal Magnetic Resonance Imaging, 2015.

[7] C. Stehling, R.B. Souza et al. “Loading of the knee during 3.0T MRI is associated with significantly increased medial meniscus extrusion in mild and moderate osteoarthritis.” European Journal of Radiology, 2012.

[8] N.E. Calixto, K. Subburaj et al. “Zonal differences in meniscus MR relaxation times in response to in vivo static loading in knee osteoarthritis.” Journal of Orthopaedic Research, 2016.

[9] S. Jerban, E. Chang and J. Du. “Magnetic resonance imaging (MRI) studies of knee joint under mechanical loading: Review.” Elsevier, 2020.

[10] C.Heilmaier et al. “A large-scale study on subjective perception of discomfort during 7 and 1.5T MRI examinations.” Bioelectromagnetics, 2011.

[11] B. Rieger, F. Zimmer, J. Zapp, S. Weingärtner and L.R. Schad. “Magnetic resonance fingerprinting using echo-planar imaging: Joint quantification of T1 and T2* relaxation times.” Magnetic Resonance in Medicine, 2017.

[12] B. Rieger, M. Akçakaya, J.C. Pariente et al. “Time efficient whole-brain coverage with MR Fingerprinting using slice-interleaved echo-planar-imaging.” Scientific Reports, 2018.

[13] T. Nishii et al. “Change in knee cartilage T2 in response to mechanical loading.” Journal of Magnetic Resonance Imaging, 2008.

[14] D. Nag et al. “Quantification of T2 relaxation changes in articular cartilage with in situ mechanical loading of the knee.” Journal of Magnetic Resonance Imaging, 2004.

[15] H. Hamada et al. “ Comparison of load responsiveness of cartilage T1rho and T2 in porcine knee joints: an experimental loading MRI study”. Osteoarthritis Research Society International, 2015.

[16] H.M. James, “Theory of the Elastic Properties of Rubber”. The Journal of Chemical Physics, 1943.